

Structure–Activity Relationship and Biological Investigation of SR18292 (16), a Suppressor of Glucagon-Induced Glucose Production

Hua Lin, Kfir Sharabi, Li Lin, Claudia Ruiz, Di Zhu, Michael D. Cameron, Scott J. Novick, Patrick R. Griffin, Pere Puigserver, and Theodore M. Kamenecka*

Cite This: *J. Med. Chem.* 2021, 64, 980–990

Read Online

ACCESS |



Metrics & More

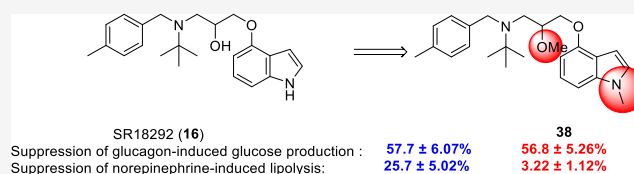


Article Recommendations



Supporting Information

ABSTRACT: Despite a myriad of available pharmacotherapies for the treatment of type 2 diabetes (T2D), challenges still exist in achieving glycemic control. Several novel glucose-lowering strategies are currently under clinical investigation, highlighting the need for more robust treatments. Previously, we have shown that suppressing peroxisome proliferator-activated receptor gamma coactivator 1-alpha activity with a small molecule (SR18292, **16**) can reduce glucose release from hepatocytes and ameliorate hyperglycemia in diabetic mouse models. Despite structural similarities in **16** to known β -blockers, detailed structure–activity relationship studies described herein have led to the identification of analogues lacking β -adrenergic activity that still maintain the ability to suppress glucagon-induced glucose release from hepatocytes and ameliorate hyperglycemia in diabetic mouse models. Hence, these compounds exert their biological effects in a mechanism that does not include adrenergic signaling. These probe molecules may lead to a new therapeutic approach to treat T2D either as a single agent or in combination therapy.



INTRODUCTION

The epidemic prevalence of type 2 diabetes (T2D) requires the development of new anti-diabetic drugs to ameliorate hyperglycemia. Targeting the liver is an attractive approach as uncontrolled hepatic glucose production (HGP) is a main contributor to the hyperglycemia observed in T2D and is a result of the reduced ability of insulin to suppress HGP.^{1–3} Commonly used anti-diabetic drugs currently include metformin, sulfonylureas, thiazolidinediones (TZDs), incretin mimetics, DPP4 antagonists,⁴ and sodium-glucose cotransporter 2 (SGLT2) inhibitors,⁵ where each drug targets a different regulatory component of glucose homeostasis. Importantly, several studies have demonstrated that increased hepatic gluconeogenesis, rather than glycogenolysis, is the primary reason for the elevated HGP and the subsequent hyperglycemia in T2D patients.^{6,7} Thus, targeting components within the HGP process, and specifically gluconeogenesis, is considered a useful way to normalize blood glucose concentrations. Accordingly, the first-line drug for T2D treatment is the biguanide metformin, which reduces blood glucose concentration primarily by suppressing gluconeogenesis and HGP.^{8–10} This highlights the possibility that new drugs that will also target gluconeogenic components might also serve as anti-diabetic agents.

The transcription coactivator peroxisome proliferator-activated receptor gamma coactivator 1-alpha (PGC-1 α) has been shown to significantly control hepatic gluconeogenesis by promoting expression of critical enzymes in the gluconeogenic

pathway.^{11–13} Modulating the acetylation status of PGC-1 α can potentially affect its gluconeogenic activity. Manipulations that augment PGC-1 α lysine acetylation have been shown to inhibit its pro-gluconeogenic activity and reduce HGP, ameliorating diabetic symptoms.^{14–17} We have previously designed a high-throughput AlphaLISA screen to discover small molecules that induce PGC-1 α acetylation with the goal that hits from this screen will ultimately suppress HGP.¹⁸ We identified a set of small molecules that can induce PGC-1 α acetylation, suppress expression of gluconeogenic genes, and reduce glucose secretion from cultured primary hepatocytes.¹⁸ We further showed that an analogue of a single hit from this screen, **16**, can potentially improve whole body insulin sensitivity. This is achieved by specifically improving the liver's response to insulin without changing glucose uptake. Although the direct target of **16** is still not known and its inhibitory effect on PGC-1 α is probably indirect, its specificity toward suppression of HGP makes it a promising chemical scaffold that can potentially be used as an anti-diabetic drug.

Received: August 20, 2020

Published: January 12, 2021



Here, we performed a structure–activity relationship (SAR) study of **16** in order to dissect in more detail the structural elements required to elicit biological activity. The conclusions from this study will help design probes that can be further used to find a direct target for **16**. In addition, **16** contains a pharmacophore similar to that of several β -adrenergic receptor (β -AdR) antagonists and is especially related to pindolol.^{19,20} However, most commercial β -blockers are secondary amino alcohols, wherein **16** contains a tertiary amine (Figure 1). This

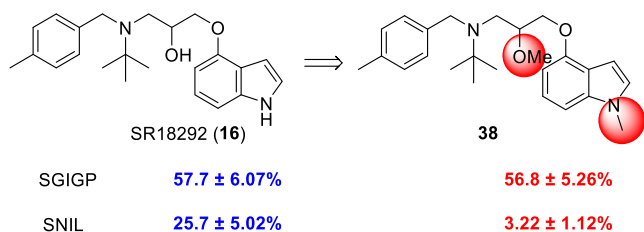
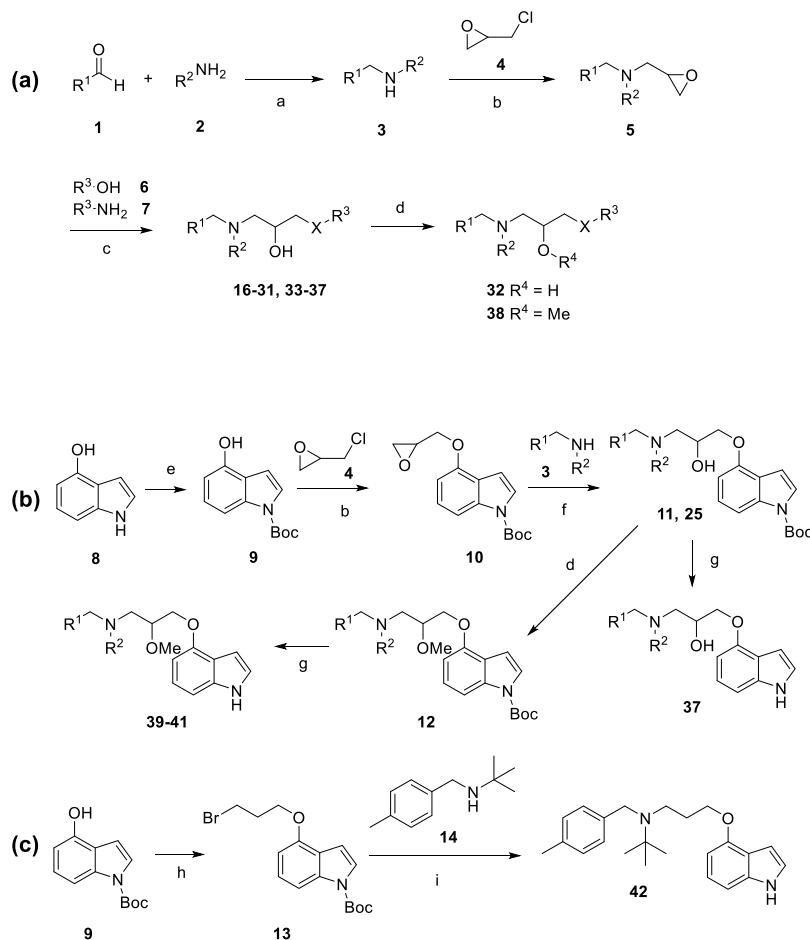


Figure 1. SAR study of **16** led to **38**.

likely reduces some of the effects at the β -adrenergic receptor but not at the molecule's direct target. We counter-screened **16** in a panel of ~50 G protein-coupled receptors, ion channels, and transporters and identified only a few off-target effects.²¹

Scheme 1. Synthesis of **16** Analogues^a



^aReaction conditions: (a) NaBH₄, MeOH, 0 °C → rt; (b) K₂CO₃, KI, CH₃CN, 80 °C; (c) K₂CO₃, DMF, 130 °C; (d) MeI, NaH, DMF, 0 °C → rt; (e) (1) BOC₂O, 4-DMAP, CH₃CN, rt; (2) K₂CO₃, MeOH, rt; (f) toluene, 130 °C; (g) Et₂NH, toluene, 150 °C; (h) 1,3-dibromopropane, NaH, DMF, 0 °C → rt; (i) i-PrOH, 120 °C.

Not surprisingly, **16** had reasonable binding to β -adrenergic receptors (β_1 K_i = 0.80 μ M; β_2 K_i = 1.3 μ M) and also weak affinity for SHT1a (K_i = 2.1 μ M). We show here that the anti-diabetic effects of **16**, both *in vitro* and *in vivo*, can be uncoupled from its β -AdR antagonist effects, suggesting that **16** improves diabetic symptoms in a mechanism that does not involve inhibition of adrenergic signaling. Moreover, we identified one analogue, **38**, with excellent bioactivity lacking β -AdR activity that can potentially be used for the potential treatment of T2D. Key modifications are shown in red (Figure 1).

RESULTS AND DISCUSSION

Most analogues could be synthesized following the general protocol as outlined in Scheme 1a. Selected analogues were made as described in Scheme 1b,c. Reductive amination of commercially available aldehydes **1** with the corresponding amines **2** afforded secondary amines **3**.

Treatment with 2-(chloromethyl)oxirane **4** in the presence of K₂CO₃ gave tertiary amines **5**. Ring opening with phenols or amines provided α -amino alcohol final products (**16–31**, **33–37**). O-alkylation with iodomethane afforded ethers **32** and **38**. Boc protection of 4-hydroxyindole **8**, followed by O-alkylation, led to oxirane intermediate **10**. Ring opening by secondary

amines **3** gave α -amino alcohols **11**, which were methylated and deprotected to provide the desired ether compounds **39–41**. Finally, Boc-protected 4-hydroxyindole **9** was O-alkylated to provide bromide **13**, which could then be treated with amine **14** to give amine **15**. Deprotection of the indole gave **42**.

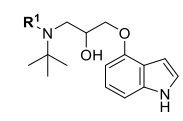
To determine the ability of the **16** analogues to suppress glucose secretion, we used isolated mouse primary hepatocytes. Upon fasting, elevated secretion of glucagon from pancreatic α -cells stimulates HGP to maintain normal blood glucose concentration when nutrients are limited.^{3,22} To induce secretion of glucose from cultured primary hepatocytes, we stimulated them with glucagon, which mimics the fasting response, and used pyruvate and lactate as substrates for glucagon-induced gluconeogenesis. As previously reported,¹⁸ **16** suppresses the glucagon-induced glucose secretion to the media by \sim 58% when pyruvate and lactate are used as substrates (Table 1, **16**). In addition, as predicted by its molecular structure, **16** was also able to suppress lipolysis in cultured adipocytes by \sim 26%, as measured by glycerol release to the medium although to a much lesser extent when compared to propranolol, a potent antagonist of β -AdR (Table 1, Pro). While we do not know the direct target of these compounds, the functional phenotypic assays described herein are fully capable of driving SAR toward compounds that suppress glucagon-induced glucose production. Initial studies began with examining the western portion of the molecule. Moving the 4-methyl group in **16** around the ring had little effect on suppression of glucagon-induced glucose production (SGIGP) or suppression of norepinephrine-induced lipolysis (SNIL) (**17–18**). Attempts to replace the 4-methyl group with alternate substituents similarly had little effect on SGIGP (**19–22, 24**); however, there was an increasing trend in inhibiting lipolysis relative to the parent (**16**). A very bulky substituent at the 4-position (**23**) did not have much effect on SGIGP; however, it did appear to reduce effects on lipolysis. Interestingly, a secondary amine ($R^1 = H$, **25**) had little effect on glucose production but the greatest effect on lipolysis inhibition almost rivaling propranolol.

We next turned our attention to the other substituent on the nitrogen atom in the linker (Table 2). Decreasing the size of the substituent from *t*-butyl (**16**) to isopropyl (**35**) to cyclopropyl was not beneficial with regard to inhibiting glucagon-induced glucose release from hepatocytes. Removing the group altogether (**37**) reduced activity even further. While **36** had reduced inhibition on lipolysis, it came with reduced activity on glucose release as well.

Modifications to the eastern portion of the molecule are highlighted in Table 3. Attaching the molecule to the 5-position of the indole ring as in **26** did little more than increasing inhibition of lipolysis. Replacement of indole with simple phenyl rings (**27, 28**) was detrimental to activity in suppressing glucose secretion, and the naphthyl analogue (**29**) completely ablated activity. A pyridine ring substitution (**30**) was moderately tolerated, as was *N*-acetylated phenol **31**, but neither was as active as **16**. *N*-Methyl indole derivative **32** retained similar activity to **16**, indicating that NH was not required as a hydrogen bond donor for activity. Attempts to replace the ether link at C4 of the indole with NH were marginally successful (**33–34**), although analogues were less active than **16**.

During the synthesis of *N*-methylindole analogue **32**, the bis-methylated analogue **38** could be isolated as a major byproduct in the presence of the excess methylating reagent (Figure 1).

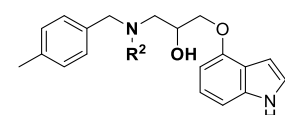
Table 1. Suppression of Glucagon-Induced Glucose Production in Hepatocytes and NE-Induced Lipolysis in Adipocytes by the Different Compounds^a



#	R ¹	SGIGP	SNIL
Pro	-	-	92.4±0.96%
16		57.7±6.0%	25.8±5.0%
17		62.6±13.6%	40.4±0.26%
18		46.0±4.9%	35.6±3.98%
19		30.1±5.24%	58.3±3.01%
20		35.5±6.2%	65.2±0.80%
21		52.2±7.9%	55.3±4.41%
22		49.3±4.8%	53.7±6.86%
23		47.3±9.7%	11.3±3.39%
24		48.5±9.0%	51.3±1.4%
25	H	53.0±2.80%	73.2±0.76%

^aThe difference between glucagon- or NE-stimulated cells and non-stimulated cells is considered as 100% suppression. Data are shown as mean \pm standard error of the mean (SEM), $n = 3–6$ /group. For both SGIGP and SNIL, the compound concentration is 1 μ M.

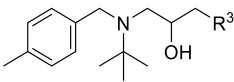
Table 2. Suppression of Glucagon-Induced Glucose Production and NE-Induced Lipolysis is Shown as % Suppression of the Glucagon/NE Effects^a

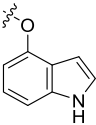
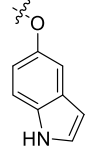
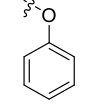
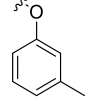
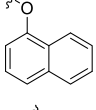
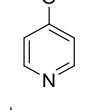
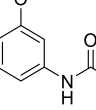
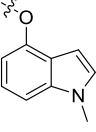
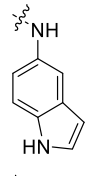


#	R ²	SGIGP (%)	SNIL (%)
16	<i>t</i> -Bu	57.7 \pm 6.07	25.8 \pm 5.02
35	<i>i</i> -Pr	59.5 \pm 9.31	51.6 \pm 2.38
36	cyclopropyl	37.8 \pm 5.55	11.6 \pm 3.28
37	H	34.5 \pm 3.73	40.6 \pm 0.64

^aThe basal non-stimulated state is considered as 100% suppression. Data are shown as mean \pm SEM, $n = 3–6$ /group. For both SGIGP and SNIL, the compound concentration is 1 μ M.

Table 3. Suppression of Glucagon-Induced Glucose Production and NE-Induced Lipolysis is Shown as % Suppression of the Glucagon/NE Effects^a



#	R ³	SGIGP	SNIL
16		57.7±6.07%	25.8±5.02%
26		50.7±8.01%	48.5±1.67%
27		32.3±7.43%	21.7±4.20%
28		31.5±11.8%	13.1±4.70%
29		-2.73±4.82%	10.4±6.25%
30		41.4±8.00%	31.5±1.76%
31		35.9±4.97%	12.3±0.56%
32		47.7±9.54%	36.7±1.47%
33		28.2±4.00%	2.24±2.36%
34		35.1±4.50%	13.2±3.30%

^aThe basal, non-stimulated state is considered as 100% suppression. Data are shown as mean ± SEM, *n* = 3–6/group. For both SGIGP and SNIL, the compound concentration is 1 μM.

The *O*-methyl ether retained activity of the parent **16** on inhibiting glucagon-stimulated glucose secretion but nearly completely abolished inhibition of lipolysis. This is perhaps not surprising given the preference for a free amino alcohol pharmacophore for β-adrenergic activity.^{23,24}

Scatter plot analysis of the data obtained to date indicated little to no correlation between the abilities of a compound to reduce glucose secretion in hepatocytes and suppress lipolysis in adipocytes (Figure 2). Importantly, the ability of two

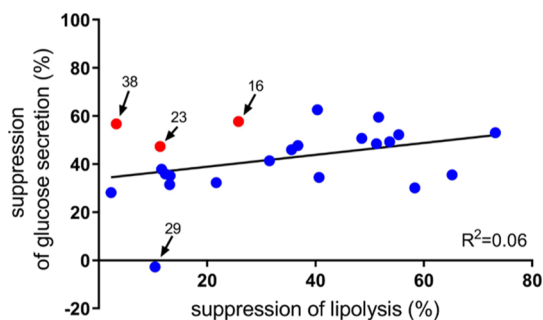


Figure 2. Data from Tables 1–3 presented as a scatter plot correlation between SNIL and SGIGP.

compounds (**38** and **23**) to suppress lipolysis was largely lost, while still retaining the ability to reduce glucose secretion from hepatocytes, similar to the parent compound (**16**) (Figure 2).

A more detailed analysis of the β-AdR antagonistic effect of **16** clearly shows that it is a weak antagonist compared to a classical β-AdR antagonist like propranolol (Figure 3A). In accordance with this, **16** does not reduce the phosphorylation of hormone-sensitive lipase (HSL) in the fat tissue isolated from fasted mice that have been treated with **16** (Figure 3B). Phosphorylation of HSL is the major molecular pathway by which adrenergic signaling promotes lipolysis from the adipose tissue,²⁵ and the lack of change in HSL phosphorylation supports the idea that **16** does not act as a β-AdR antagonist *in vivo*. Moreover, inhibition of adrenergic signaling in the liver is expected to result in inhibition of glycogenolysis and accumulation of liver glycogen.²⁶ While their blood glucose concentration is significantly lower, fasted mice that have been treated with **16** do not show increased accumulation of liver glycogen compared to vehicle-treated mice (Figure 3C,D), providing further support that **16** does not act as a β-AdR antagonist *in vivo*.

To better compare the β-AdR antagonistic effect of **16** and its analogues **38** and **23**, we generated a dose response curve and showed that **38** and **23** lose β-AdR antagonistic activity in cultured adipocytes in a wide range of concentrations (Figure 4A). Overexpression of PGC-1α in hepatocytes is sufficient to promote glucose release (Figure 4B), even without glucagon stimulation, highlighting its important contribution to this process. **38** was able to inhibit the PGC-1α-driven glucose release, similar to **16**, implying that both analogues inhibit glucose release through a mechanism that involves inhibition of PGC-1α activity. Importantly, **38** and **23** retain their ability to reduce fasting blood glucose in diabetic mice (Figure 4C), providing additional evidence that the β-AdR antagonistic effect of **16** is uncoupled from its anti-diabetic effects. Moreover, similar to **16**, mice that have been treated with **23** do not show reduced phosphorylation of HSL in the fat tissue or accumulation of liver glycogen (Figure 4D,E), which is consistent with no β-AdR antagonism *in vivo*.

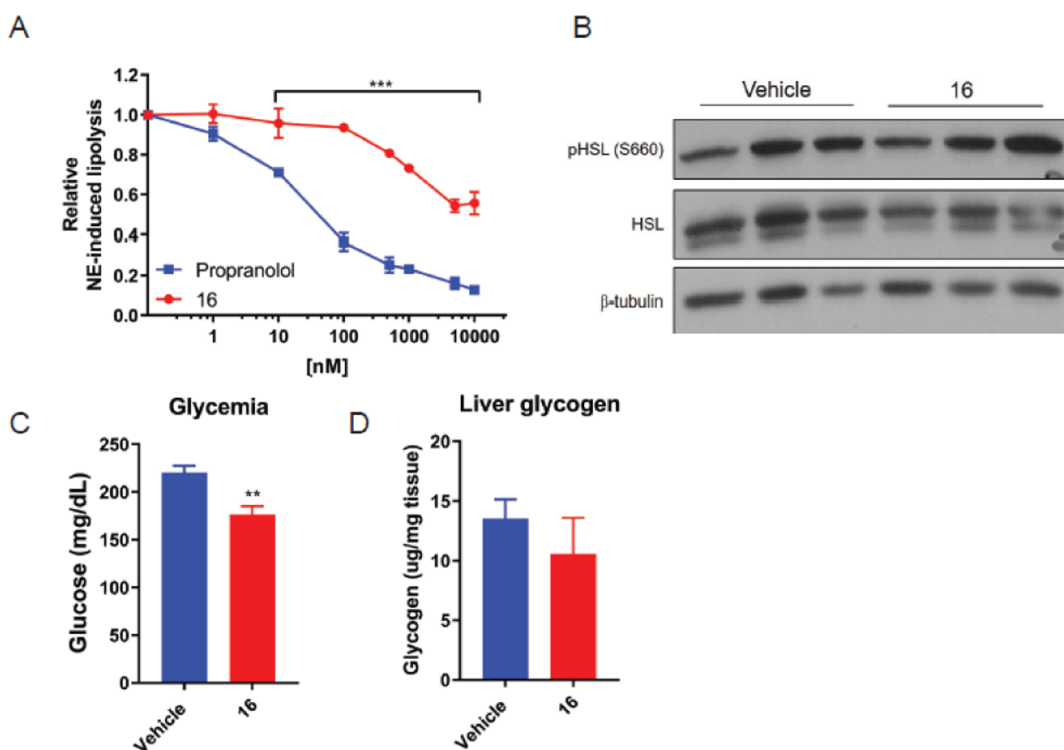


Figure 3. (A) Fully differentiated cultured brown adipocytes were treated with either **16** or propranolol at the indicated dose for 30 min, followed by NE stimulation (1 μ M) for 90 min. Media were collected, and glycerol levels were measured. For each dose, $n = 3$; ***, $P < 0.001$; two-way ANOVA. (B) HSL phosphorylation level is not altered in the epididymal white adipose tissue collected from mice fed with HFD for 2 months and treated with **16** (50 mg/kg). (C) Fasting Blood glucose (6 h fast) and (D) hepatic glycogen levels in HFD mice treated with **16**. $n = 4/5$, vehicle/**16**; **, $P < 0.01$; two-tailed t -test.

Following up on **38**, we were curious to characterize the simple *O*-methyl ether analogue of **16** given that *N*-methylation of the indole was not productive (**32**, Table 3). Surprisingly, this compound had more than twofold improvement in suppressing glucagon-stimulated glucose production relative to **38** as well as **16**, while retaining little to no activity on inhibiting lipolysis (**39**, Table 4). Further investigation of the western portion of the molecule exhibited similar SAR as in the **16** series with the best substitution as a cyclopentylmethyl group (**41**) exhibiting a similar suppression of SGIGP relative to **16** with no effect on lipolysis. The analogue lacking the *O*-methyl ether (**42**) altogether was considerably less potent, emphasizing the importance of this substituent for activity. Nonetheless, analogues such as **38** and **41** highlight the ability to completely dissociate the ability to suppress glucose secretion from β -adrenergic activity.

CONCLUSIONS

Here, we describe the synthesis and SAR of **16** and its analogues. Starting with a weak β -adrenergic receptor scaffold, we were able to modify specific portions of the molecule to optimize anti-gluconeogenic potential as well as minimize β -adrenergic antagonist activity as measured via lipolysis both *in vitro* and *in vivo*. Reducing the β -adrenergic activity of **16** is important as β -blockers are commonly used to treat hypertension and related heart problems, which can complicate the therapeutic usage of this small molecule. Ablation of β -adrenergic activity was accomplished by *O*-methylation of the secondary alcohol, a known requirement for β -blocking efficacy. Our exploration uncoupled the anti-gluconeogenic effect of **16** from its β -AdR blocking effect and generated useful

probes that can be further used to understand **16**'s mechanism of action. These studies are currently underway now that selective inhibitors such as **38** have been identified and will be reported in due course.

EXPERIMENTAL SECTION

Chemistry. All solvents and chemicals were of reagent grade. Unless otherwise mentioned, all reagents and solvents were purchased from commercial vendors and used as received. Flash column chromatography was carried out on a Teledyne ISCO CombiFlash R_f system using prepacked columns. Solvents used include hexane, ethyl acetate (EtOAc) (EA), dichloromethane (DCM), and methanol. The purity and characterization of compounds were established by a combination of HPLC, thin-layer chromatography (TLC), mass spectrometry, and NMR analyses. ^1H and ^{13}C NMR spectra were recorded on a Bruker AVANCE DPX-400 (400 MHz), a Bruker UltraShield 500 Plus, and an AVANCE III 600 (600 MHz) spectrometer and were determined in chloroform- d or DMSO- d_6 with solvent peaks as the internal reference. Chemical shifts are reported in parts per million (ppm) relative to the reference signal, and coupling constant (J) values are reported in hertz (Hz). TLC was performed on EMD precoated silica gel 60 F254 plates, and spots were visualized with UV light or iodine staining. Low-resolution mass spectra were recorded using a Thermo Scientific Ultimate 3000/LCQ Fleet system (ESI). High-resolution mass spectra were recorded using a Thermo Scientific EXACTIVE system (ESI). All compounds containing a stereogenic center are racemic. All test compounds were greater than 95% pure as determined using an Agilent 1100 series HPLC using a Supelco Discovery HS C18 10 cm \times 2.1 mm, 5 μ m column or an Agilent 1260 Infinity II using an Agilent ZORBAX SB C18 250 mm \times 4.6 mm, 5 μ m column.

General Procedure for the Synthesis of **3a–3d and **3f–3k**.** To a room-temperature solution of aldehyde **1** (1 equiv) in MeOH was added amine **2** (1.2 equiv). The solution was stirred at room

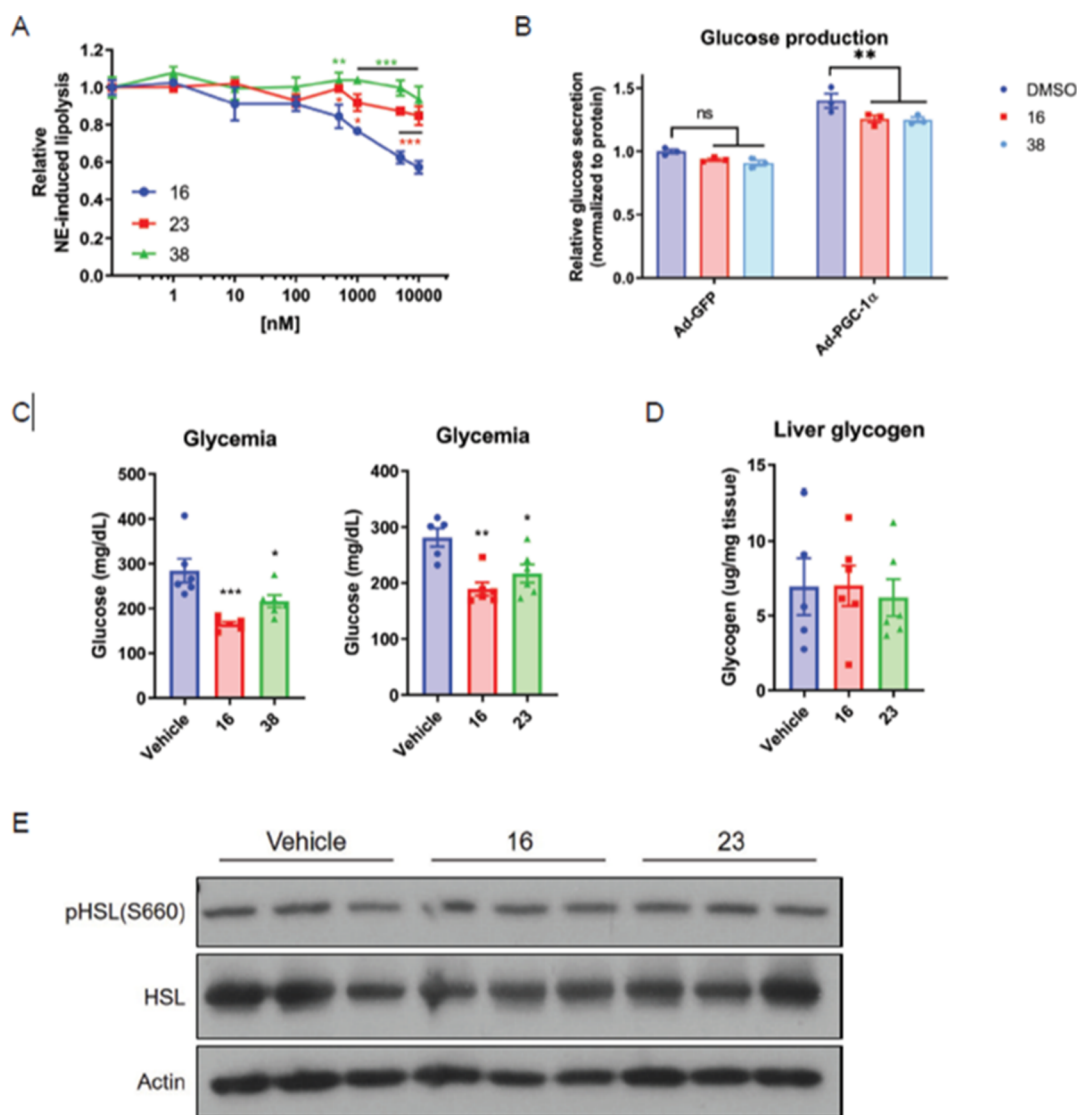


Figure 4. (A) Fully differentiated cultured brown adipocytes were treated with **16**, **23**, or **38** at the indicated dose for 30 min, followed by NE stimulation ($1 \mu\text{M}$) for 90 min. Media were collected, and glycerol levels were measured. For each dose, $n = 3$; **, $P < 0.01$, ***, $P < 0.001$; two-way ANOVA. (B) Overexpression of PGC-1 α using adenoviral vectors promotes glucose release from primary hepatocytes. **16** and **38** ($10 \mu\text{M}$) are able to inhibit the PGC-1 α -driven glucose release. (C) Fasting blood glucose (overnight fast) of ob/ob mice treated with **16**, **38**, or **23** (25 mg/kg). (D) Liver glycogen levels of ob/ob mice treated with **16** or **23** (25 mg/kg); *, $P < 0.05$, **, $P < 0.01$, one-way ANOVA. (E) HSL phosphorylation is not altered in the brown adipose tissue of ob/ob mice treated with **16** or **23** (25 mg/kg).

temperature for 1 h, cooled to $0 \text{ }^\circ\text{C}$, and then treated with NaBH_4 (1.5 equiv) in one portion. The reaction mixture was allowed to warm to room temperature overnight with stirring. The reaction mixture was quenched with water and then was concentrated. The residue was dissolved in HCl (1 N) and washed with Et_2O . The water phase was basified with NaOH (1 N) until pH > 10 , extracted with DCM, washed with brine, dried (Na_2SO_4), and concentrated *in vacuo* to give the desired secondary amine **3** which was used for the next step without any further purification.

General Procedure for the Synthesis of 5a–k. To a solution of amine **3** (1 equiv) in acetonitrile were added 2-(chloromethyl)-oxirane **4** (3 equiv), K_2CO_3 (3 equiv), and KI (3 equiv). The mixture was heated to $80 \text{ }^\circ\text{C}$ for 16 h, cooled, and filtered, washing with EA. The filtrate was concentrated *in vacuo* and purified by flash chromatography on silica gel [EtOAc/petroleum ether (PE)] to afford amine **5** as a colorless oil.

2-Methyl-N-(4-methylbenzyl)-N-(oxiran-2-ylmethyl)propan-2-amine (5a). Colorless oil, $R_f = 0.3$ (PE/EA = 10:1). ^1H NMR (600 MHz, CDCl_3): δ 1.17 (s, 9H), 2.33 (s, 3H), 3.60 (d, $J = 14.8 \text{ Hz}$, 1H), 3.83 (d, $J = 14.8 \text{ Hz}$, 1H), 7.09 (t, $J = 3.0 \text{ Hz}$, 1H), 7.10 (d, $J =$

7.8 Hz, 2H), 7.28 (d, $J = 7.9 \text{ Hz}$, 2H). ^{13}C NMR (600 MHz, CDCl_3): δ 139.51, 136.04, 128.86, 128.17, 54.87, 54.26, 52.83, 52.45, 47.37, 27.53, 21.19. ESI ($\text{M} + \text{H}$) $^+ = 234$.

2-Methyl-N-(3-methylbenzyl)-N-(oxiran-2-ylmethyl)propan-2-amine (5b). Colorless oil, $R_f = 0.3$ (PE/EA = 10:1). ^1H NMR (600 MHz, CDCl_3): δ 7.23–7.18 (m, 1H), 7.04 (d, $J = 7.0 \text{ Hz}$, 1H), 3.87 (d, $J = 14.8 \text{ Hz}$, 1H), 3.62 (d, $J = 14.7 \text{ Hz}$, 1H), 2.91 (dd, $J = 14.5$, 4.8 Hz, 1H), 2.81–2.77 (m, 1H), 2.51–2.47 (m, 1H), 2.36 (s, 1H), 2.13 (dd, $J = 4.9$, 2.7 Hz, 1H), 1.20 (s, 3H). ^{13}C NMR (126 MHz, CDCl_3): δ 142.47, 137.60, 128.92, 128.03, 127.30, 125.36, 54.85, 54.47, 52.79, 52.36, 47.31, 27.49, 21.54. ESI ($\text{M} + \text{H}$) $^+ = 234$.

General Procedure for the Synthesis of 16–24, 26–31, and 33–36. To a solution of amine **5** (1 equiv) in dimethylformamide (DMF) were added phenol or amine **6** (3 equiv) and K_2CO_3 (3 equiv). The mixture was heated to $130 \text{ }^\circ\text{C}$ for 12 h and then cooled. The reaction mixture was diluted with EA and washed with water. Then, the organic phase was concentrated and dissolved in DCM, washed with NaOH (1 N), brine, dried (Na_2SO_4), and concentrated *in vacuo*. The residue was purified by flash chromatography on silica

Table 4. Suppression of Glucagon-Induced Glucose Production and NE-Induced Lipolysis is Shown as % Suppression of the Glucagon/NE Effects^a

#	Compound	SGIGP	SNIL
Pro	-	-	76.4±5.71%
16		57.7±6.07%	25.8±5.02%
38		56.8±5.26%	3.22±1.12%
39		135±9.90%	-8.50±5.83%
40		22.7±3.26%	14.6±3.77%
41		66.4±2.50%	1.00±1.64%
42		28.3±4.05%	9.91±6.97%

^aThe basal, non-stimulated state is considered as 100% suppression. Data are shown as mean ± SEM, $n = 3-6$ /group. For both SGIGP and SNIL, the compound concentration is 1 μ M.

gel (DCM/EA) or by reverse-phase preparative HPLC to give the desired products **16-24**, **26-31**, and **33-36**.

1-((1H-Indol-4-yl)oxy)-3-(tert-butyl(4-methylbenzyl)amino)propan-2-ol (16). Off-white solid, $R_f = 0.3$ (DCM/EA = 3:1). ¹H NMR (600 MHz, CDCl₃): δ 8.23 (s, 1H), 7.27 (d, $J = 9.5$ Hz, 2H), 7.15 (d, $J = 9.3$ Hz, 2H), 7.10 (t, $J = 3.6$ Hz, 1H), 7.08 (t, $J = 9.4$ Hz, 1H), 7.01 (d, $J = 9.8$ Hz, 1H), 6.64 (td, $J = 2.6, 0.9$ Hz, 1H), 6.42 (d, $J = 9.1$ Hz, 1H), 3.96 (dd, $J = 11.5, 6.1$ Hz, 1H), 3.93 (dd, $J = 11.5, 6.1$ Hz, 1H), 3.88 (d, $J = 17.2$ Hz, 1H), 3.64 (dd, $J = 16.7, 6.2$ Hz, 1H), 3.62 (d, $J = 17.4$ Hz, 1H), 2.92 (dd, $J = 16.4, 10.6$ Hz, 1H), 2.85 (dd, $J = 16.4, 6.0$ Hz, 1H), 2.36 (s, 3H), 1.24 (s, 9H). ¹³C NMR (126 MHz, CDCl₃): δ 152.67, 138.90, 137.40, 136.59, 129.33, 128.39, 122.80, 122.63, 118.85, 104.62, 100.78, 100.06, 70.43, 67.54, 55.86, 55.59, 54.11, 27.60, 21.23. HRMS (ESI⁺) m/z : [M + H]⁺, calcd for C₂₃H₃₁N₂O₂⁺, 367.2380; found, 367.2398.

1-((1H-Indol-4-yl)oxy)-3-(tert-butyl(3-methylbenzyl)amino)propan-2-ol (17). Off-white solid, $R_f = 0.3$ (DCM/EA = 3:1). ¹H NMR (600 MHz, CDCl₃): δ 8.24 (s, 1H), 7.23 (t, $J = 7.2$ Hz, 1H), 7.19 (d, $J = 7.2$ Hz, 1H), 7.17 (d, $J = 7.2$ Hz, 1H), 7.08 (t, $J = 7.1$ Hz, 1H), 7.06 (d, 7.1 Hz, 1H), 7.05 (d, 7.1 Hz, 1H), 6.62 (s, 1H), 6.41 (d, $J = 6.4$ Hz, 1H), 3.95 (m, $J = 3.9$ Hz, 2H), 3.86 (d, $J = 3.9$ Hz, 1H), 3.65 (dd, $J = 3.6$ Hz, 1H), 3.62 (d, $J = 3.62$ Hz, 1H), 2.91 (dd, $J = 2.9$ Hz, 1H), 2.85 (dd, $J = 2.9$ Hz, 1H), 2.36 (s, 3H), 1.22 (s, 9H). ¹³C NMR (126 MHz, CDCl₃): δ 152.64, 142.01, 138.14, 137.38, 129.11, 128.51, 127.81, 125.47, 122.76, 122.66, 118.81, 104.65, 100.72, 99.98,

70.39, 67.57, 55.88, 54.26, 29.83, 27.58, 21.58. HRMS (ESI⁺) m/z : [M + H]⁺, calcd for C₂₃H₃₁N₂O₂⁺, 367.2380; found, 367.2394.

1-((1H-Indol-5-yl)oxy)-3-(tert-butyl(4-methylbenzyl)amino)propan-2-ol (26). Off-white solid, $R_f = 0.3$ (DCM/EA = 3:1). ¹H NMR (500 MHz, CDCl₃): δ 8.15 (s, 1H), 7.25-7.21 (m, 3H), 7.15 (t, $J = 2.8$ Hz, 1H), 7.12 (d, $J = 7.7$ Hz, 2H), 7.01 (d, $J = 2.4$ Hz, 1H), 6.81 (dd, $J = 8.8, 2.4$ Hz, 1H), 6.45 (t, $J = 2.7$ Hz, 1H), 3.86 (d, $J = 14.4$ Hz, 1H), 3.81 (d, $J = 5.1$ Hz, 2H), 3.61-3.52 (m, 2H), 2.88-2.73 (m, 2H), 2.33 (s, 3H), 1.20 (s, 9H). ¹³C NMR (126 MHz, CDCl₃): δ 153.49, 138.89, 136.53, 131.19, 129.30, 128.30, 124.96, 112.89, 111.67, 103.59, 102.41, 71.32, 67.45, 55.83, 55.53, 54.00, 27.58, 21.22. HRMS (ESI⁺) m/z : [M + H]⁺, calcd for C₂₃H₃₁N₂O₂⁺, 367.2380; found, 367.2394.

1-(tert-Butyl(4-methylbenzyl)amino)-3-phenoxypropan-2-ol (27). Off-white solid, $R_f = 0.3$ (DCM/EA = 3:1). ¹H NMR (600 MHz, chloroform-*d*): δ 10.84 (s, 1H), 7.41 (d, $J = 7.6$ Hz, 2H), 7.26 (t, $J = 7.9$ Hz, 2H), 7.14 (d, $J = 7.4$ Hz, 2H), 6.95 (t, $J = 7.3$ Hz, 1H), 6.74 (d, $J = 7.8$ Hz, 2H), 4.69 (d, $J = 12.1$ Hz, 1H), 3.75 (d, $J = 12.2$ Hz, 1H), 3.68 (d, $J = 9.2$ Hz, 1H), 3.58 (t, $J = 8.4$ Hz, 1H), 3.31 (d, $J = 12.9$ Hz, 2H), 3.27-3.17 (m, 1H), 2.30 (s, 3H), 1.58 (s, 9H). ¹³C NMR (151 MHz, CDCl₃): δ 158.29, 140.54, 132.05, 130.05, 129.63, 125.58, 121.24, 114.34, 69.61, 65.43, 64.87, 55.00, 25.33, 21.41. HRMS (ESI⁺) m/z : [M + H]⁺, calcd for C₂₁H₃₀NO₂⁺, 328.2271; found, 328.2283.

1-((1H-Indol-5-yl)amino)-3-(tert-butyl(4-methylbenzyl)amino)propan-2-ol (33). Off-white solid, $R_f = 0.2$ (DCM/EA = 3:1). ¹H

NMR (500 MHz, CDCl₃): δ 7.97 (s, 1H), 7.24 (s, 1H), 7.22 (s, 1H), 7.14 (t, J = 8.0 Hz, 3H), 7.08 (t, J = 2.8 Hz, 1H), 6.76 (d, J = 2.2 Hz, 1H), 6.54 (dd, J = 8.6, 2.2 Hz, 1H), 6.38–6.37 (m, 1H), 3.85 (d, J = 14.2 Hz, 1H), 3.55 (d, J = 14.3 Hz, 2H), 3.42 (tt, J = 7.8, 3.1 Hz, 1H), 3.13 (dd, J = 11.9, 3.8 Hz, 1H), 2.92–2.82 (m, 2H), 2.61 (dd, J = 13.6, 4.1 Hz, 1H), 2.34 (s, 3H), 1.20 (s, 9H). ¹³C NMR (126 MHz, CDCl₃): δ 142.77, 138.75, 136.60, 130.20, 129.33, 128.83, 128.35, 124.38, 112.66, 111.59, 102.45, 101.82, 67.15, 55.83, 55.51, 54.54, 49.01, 27.59, 21.22. HRMS (ESI⁺) m/z : [M + H]⁺, calcd for C₂₃H₃₂N₃O⁺, 366.2540; found, 366.2555.

1-((1H-Indol-7-yl)amino)-3-(tert-butyl(4-methylbenzyl)amino)propan-2-ol (34). Off-white solid, R_f = 0.2 (DCM/EA = 3:1). ¹H NMR (500 MHz, CDCl₃): δ 8.58 (s, 1H), 7.23 (d, J = 8.0 Hz, 2H), 7.13 (dd, J = 14.9, 7.8 Hz, 3H), 7.01 (d, J = 2.7 Hz, 1H), 6.95 (t, J = 7.7 Hz, 1H), 6.47–6.45 (m, 1H), 6.36 (d, J = 7.6 Hz, 1H), 3.81 (d, J = 14.2 Hz, 2H), 3.58 (d, J = 14.1 Hz, 1H), 3.47 (d, J = 3.4 Hz, 1H), 3.23 (dd, J = 12.6, 3.1 Hz, 1H), 2.95–2.84 (m, 2H), 2.61 (dd, J = 13.6, 4.3 Hz, 1H), 2.36 (s, 3H), 1.22 (d, J = 1.4 Hz, 9H). ¹³C NMR (126 MHz, CDCl₃): δ 138.59, 136.77, 134.47, 129.38, 128.57, 128.53, 126.95, 123.51, 120.47, 111.77, 104.56, 103.00, 67.48, 55.97, 55.59, 53.77, 48.13, 27.58, 21.27. HRMS (ESI⁺) m/z : [M + H]⁺, calcd for C₂₃H₃₂N₃O⁺, 366.2540; found, 366.2555.

1-(tert-Butyl(4-methylbenzyl)amino)-3-((1-methyl-1H-indol-4-yl)oxy)propan-2-ol (32). To a solution of **16** (1 equiv) in THF cooled to 0 °C was added NaH (1.5 equiv) in one portion. After stirring at 0 °C for 1 h, MeI (1 equiv) was added. The mixture was allowed to warm to room temperature overnight with stirring. The reaction mixture was quenched with saturated aqueous NH₄Cl solution and extracted with EA. The organic layer was washed with saturated sodium bicarbonate solution, brine, dried (Na₂SO₄), and concentrated *in vacuo*. The crude residue was purified on silica gel (DCM/EA) to give the desired product **32** as an off-white solid. ¹H NMR (500 MHz, CDCl₃): δ 7.25–7.23 (m, 1H), 7.15–7.08 (m, 3H), 6.97–6.92 (m, 2H), 6.56 (d, J = 3.1 Hz, 1H), 6.41 (d, J = 7.7 Hz, 1H), 3.97–3.88 (m, 2H), 3.85 (d, J = 14.4 Hz, 1H), 3.77 (s, 3H), 3.62 (td, J = 9.7, 5.0 Hz, 2H), 2.86 (qd, J = 14.0, 7.0 Hz, 2H), 2.35 (s, 3H), 1.22 (s, 10H). ¹³C NMR (126 MHz, CDCl₃): δ 152.70, 138.95, 138.35, 136.55, 129.32, 128.37, 127.26, 122.39, 119.27, 102.85, 100.50, 98.47, 70.46, 67.55, 55.85, 55.57, 54.19, 33.14, 27.59, 21.23. HRMS (ESI⁺) m/z : [M + H]⁺, calcd for C₂₄H₃₃N₂O₂⁺, 381.2537; found, 381.2551.

N-(tert-Butyl)-2-methoxy-3-((1-methyl-1H-indol-4-yl)oxy)-N-(4-methylbenzyl)propan-1-amine (38). To a solution of **16** (1 equiv) in THF cooled to 0 °C was added NaH (3 equiv) in one portion. After stirring at 0 °C for 1 h, MeI (3 equiv) was added. The mixture was allowed to warm to room temperature overnight with stirring. The reaction mixture was quenched with saturated aqueous NH₄Cl solution and extracted with EA. The organic layer was washed with saturated sodium bicarbonate solution, brine, dried (Na₂SO₄), and concentrated *in vacuo*. The crude residue was purified on silica gel (DCM/EA) to give the desired product **38** as an off-white solid. ¹H NMR (500 MHz, CDCl₃): δ 7.42–7.37 (m, 2H), 7.27–7.21 (m, 3H), 7.09–7.05 (m, 2H), 6.69 (dd, J = 3.1, 0.8 Hz, 1H), 6.49 (d, J = 7.7 Hz, 1H), 4.26 (dd, J = 10.0, 3.3 Hz, 1H), 3.97 (dd, J = 10.1, 6.0 Hz, 1H), 3.89 (s, 3H), 3.88–3.85 (m, 2H), 3.53 (s, 3H), 3.50 (ddt, J = 8.5, 5.6, 2.7 Hz, 1H), 3.02 (dd, J = 13.9, 8.2 Hz, 1H), 2.90 (dd, J = 14.0, 5.2 Hz, 1H), 2.47 (s, 3H), 1.28 (s, 9H). ¹³C NMR (126 MHz, CDCl₃): δ 152.93, 140.07, 138.33, 135.98, 128.96, 128.29, 127.10, 122.35, 119.41, 102.58, 100.39, 98.72, 80.07, 69.16, 58.37, 55.72, 55.65, 52.62, 33.13, 27.41, 21.20. HRMS (ESI⁺) m/z : [M + H]⁺, calcd for C₂₅H₃₅N₂O₂⁺, 395.2693; found, 395.2708.

tert-Butyl 4-Hydroxy-1H-indole-1-carboxylate (9). To a solution of 4-hydroxyindole (**8**, 1 equiv) in acetonitrile were added di-*tert*-butyl dicarbonate (3 equiv) and dimethylaminopyridine (DMAP) (0.1 equiv). The solution was aged at room temperature for 1 h and then concentrated *in vacuo*. Solid potassium carbonate (5 equiv) was added to a solution of the crude residue in methanol, and the mixture was stirred at room temperature for 3 h. The reaction mixture was acidified with acetic acid and extracted with EA. The organic layer was washed with saturated brine and dried over anhydrous sodium sulfate.

The solvent was evaporated under reduced pressure, and the residue was purified by flash column chromatography (hexane/EA = 90:10) to obtain *tert*-butyl 4-hydroxy-1H-indole-1-carboxylate **9** as a colorless solid. ¹H NMR (600 MHz, CDCl₃): δ 7.74 (d, J = 7.3 Hz, 1H), 7.53 (d, J = 3.3 Hz, 1H), 7.16 (t, J = 8.1 Hz, 1H), 6.70–6.65 (m, 2H), 1.68 (s, 9H). ¹³C NMR (151 MHz, CDCl₃): δ 150.10, 148.89, 137.01, 125.30, 124.82, 119.82, 108.38, 107.93, 103.74, 84.04, 28.31. EI (M + H)⁺ = 234.

tert-Butyl 4-(Oxiran-2-ylmethoxy)-1H-indole-1-carboxylate (10). To a solution of **9** (1 equiv) in acetonitrile were added 2-(chloromethyl)oxirane **4** (3 equiv), K₂CO₃ (3 equiv), and KI (3 equiv). The mixture was heated to 70 °C for 16 h, cooled, and filtered, washing with EA. The filtrate was concentrated *in vacuo* and purified by flash chromatography on silica gel (EtOAc/hexanes) to afford *tert*-butyl 4-(oxiran-2-ylmethoxy)-1H-indole-1-carboxylate **10** as a colorless solid. ¹H NMR (600 MHz, CDCl₃): δ 7.78 (d, J = 7.5 Hz, 1H), 7.51 (d, J = 3.5 Hz, 1H), 7.21 (t, J = 8.1 Hz, 1H), 6.73 (d, J = 3.7 Hz, 1H), 6.66 (d, J = 7.9 Hz, 1H), 4.35 (dd, J = 11.1, 3.1 Hz, 1H), 4.09 (dd, J = 11.1, 5.6 Hz, 1H), 3.43 (ddt, J = 5.7, 4.0, 3.0 Hz, 1H), 2.94–2.92 (m, 1H), 2.80 (dd, J = 4.9, 2.7 Hz, 1H), 1.67 (s, 9H). ¹³C NMR (151 MHz, CDCl₃): δ 151.86, 149.93, 136.71, 125.09, 124.63, 121.15, 108.99, 104.42, 104.29, 83.82, 69.09, 50.35, 44.88, 28.29. EI (M + H)⁺ = 290.

General Procedure for the Synthesis of 11 or 25. A solution of **10** (1 equiv) and amine **3** (1 equiv) in toluene was heated to 130 °C overnight. The solution was cooled and concentrated *in vacuo* to purify on silica gel (DCM/EA) to afford the title compound.

tert-Butyl 4-(3-(tert-Butyl(4-methylbenzyl)amino)-2-hydroxypropoxy)-1H-indole-1-carboxylate (11a). Off-white solid, R_f = 0.3 (DCM/EA = 3:1). ¹H NMR (600 MHz, CDCl₃): δ 7.72 (d, J = 8.4 Hz, 1H), 7.47 (d, J = 3.8 Hz, 1H), 7.21 (d, J = 7.7 Hz, 2H), 7.16 (t, J = 8.1 Hz, 1H), 7.11 (d, J = 7.7 Hz, 2H), 6.64 (d, J = 3.8 Hz, 1H), 6.51 (d, J = 8.0 Hz, 1H), 3.84 (m, 3H), 3.57 (d, J = 14.4 Hz, 2H), 2.85 (m, 1H), 2.77 (dd, J = 13.7, 4.9 Hz, 1H), 2.32 (s, 3H), 1.65 (s, 9H), 1.19 (s, 11H). ¹³C NMR (126 MHz, CDCl₃): δ 152.22, 149.96, 138.74, 136.59, 129.31, 128.37, 125.09, 124.32, 121.05, 108.50, 104.49, 104.22, 83.69, 70.56, 67.42, 55.84, 55.56, 53.86, 28.29, 27.55, 21.20. ESI (M + H)⁺ = 467.

tert-Butyl 4-(3-(tert-Butyl(2-methylbenzyl)amino)-2-hydroxypropoxy)-1H-indole-1-carboxylate (11b). Off-white solid, R_f = 0.3 (DCM/EA = 3:1). ¹H NMR (600 MHz, CDCl₃): δ 7.72 (d, J = 7.0 Hz, 1H), 7.47 (d, J = 3.1 Hz, 1H), 7.40–7.38 (m, 1H), 7.17–7.13 (m, 4H), 6.63 (d, J = 3.7 Hz, 1H), 6.49 (d, J = 8.0 Hz, 1H), 3.91 (d, J = 14.1 Hz, 1H), 3.81 (dd, J = 4.8, 3.0 Hz, 2H), 3.62 (d, J = 14.1 Hz, 1H), 3.32 (dt, J = 10.0, 5.0 Hz, 1H), 2.86 (dd, J = 13.8, 8.6 Hz, 1H), 2.78 (dd, J = 13.9, 5.1 Hz, 1H), 2.38 (s, 3H), 1.66 (s, 9H), 1.22 (s, 9H). ¹³C NMR (126 MHz, CDCl₃): δ 152.21, 150.02, 138.98, 136.45, 130.62, 129.60, 127.19, 126.10, 125.13, 124.39, 121.06, 108.54, 104.48, 104.25, 70.54, 67.94, 56.15, 53.40, 53.20, 28.34, 27.25, 19.54. ESI (M + H)⁺ = 467.

tert-Butyl 4-(3-(tert-Butyl(4-methylbenzyl)amino)-2-hydroxypropoxy)-1H-indole-1-carboxylate (25). Off-white solid, R_f = 0.3 (DCM/MeOH = 10:1). ¹H NMR (600 MHz, DMSO-*d*₆): δ 11.07 (s, 1H), 7.20 (s, 1H), 6.99 (d, J = 7.8 Hz, 1H), 6.97 (t, J = 7.4 Hz, 1H), 7.21 (t, J = 7.2 Hz, 2H), 6.44 (s, 1H), 4.00–4.06 (m, 2H), 3.87–3.93 (m, 1H), 2.74 (dd, J = 11.2, 6.5 Hz, 1H), 2.64 (dd, J = 11.2, 6.5 Hz, 1H), 1.19 (s, 11H). ¹³C NMR (126 MHz, DMSO-*d*₆): δ 152.09, 137.33, 123.43, 121.74, 118.42, 104.80, 99.93, 98.38, 70.57, 68.87, 50.01, 45.38, 28.62. HRMS (ESI⁺) m/z : [M + H]⁺, calcd for C₁₅H₂₂N₂O₃⁺, 263.1754; found, 263.1763.

General Procedure for the Synthesis of 12. To a solution of **11** (1 equiv) in THF cooled to 0 °C was added NaH (1.5 equiv) in one portion. The reaction mixture was stirred at 0 °C for 1 h, and then, MeI (1.5 equiv) was added dropwise. The mixture was allowed to warm to room temperature overnight with stirring. The reaction mixture was quenched with saturated aqueous NH₄Cl solution and extracted with EA. The organic layer was washed with saturated sodium bicarbonate solution, brine, dried (Na₂SO₄), and concentrated *in vacuo*. The crude residue was purified on silica (DCM/EA) gel to give the desired product **12**.

tert-Butyl 4-(3-(tert-Butyl(4-methylbenzyl)amino)-2-methoxypropoxy)-1H-indole-1-carboxylate (12a). Off-white solid, $R_f = 0.4$ (DCM/EA = 3:1). $^1\text{H NMR}$ (600 MHz, CDCl_3): δ 7.74 (d, $J = 8.2$ Hz, 1H), 7.48 (d, $J = 3.7$ Hz, 1H), 7.24 (d, $J = 7.7$ Hz, 2H), 7.19 (t, $J = 8.1$ Hz, 1H), 7.08 (d, $J = 7.7$ Hz, 2H), 6.65 (d, $J = 3.7$ Hz, 1H), 6.48 (d, $J = 7.9$ Hz, 1H), 4.11–3.77 (m, 2H), 3.76–3.67 (m, 2H), 3.39 (s, 3H), 3.32 (dt, $J = 6.1, 3.4, 3.0$ Hz, 1H), 2.89–2.74 (m, 2H), 2.33 (s, 3H), 1.68 (s, 9H), 1.14 (s, 9H). $^{13}\text{C NMR}$ (126 MHz, CDCl_3): δ 152.47, 150.05, 139.90, 136.58, 136.09, 128.98, 128.33, 125.08, 124.21, 121.16, 108.29, 104.72, 104.20, 83.66, 79.99, 69.23, 58.36, 55.80, 55.67, 52.31, 28.33, 27.39, 21.19. ESI ($M + H$) $^+ = 481$.

tert-Butyl 4-(3-(tert-Butyl(2-methylbenzyl)amino)-2-methoxypropoxy)-1H-indole-1-carboxylate (12b). Off-white solid, $R_f = 0.4$ (DCM/EA = 3:1). $^1\text{H NMR}$ (600 MHz, CDCl_3): δ 7.72 (d, $J = 6.8$ Hz, 1H), 7.50–7.47 (m, 1H), 7.46 (d, $J = 3.2$ Hz, 1H), 7.18 (t, $J = 8.1$ Hz, 1H), 7.15–7.12 (m, 2H), 7.11 (dd, $J = 8.8, 5.1$ Hz, 1H), 6.64 (d, $J = 3.7$ Hz, 1H), 6.50 (d, $J = 7.9$ Hz, 1H), 4.06 (dd, $J = 10.0, 3.0$ Hz, 1H), 3.82 (d, $J = 14.6$ Hz, 1H), 3.78 (dd, $J = 10.0, 5.8$ Hz, 1H), 3.65 (d, $J = 14.7$ Hz, 1H), 3.29 (s, 3H), 3.07–3.03 (m, 1H), 2.90 (dd, $J = 13.9, 8.5$ Hz, 1H), 2.71 (dd, $J = 13.9, 5.0$ Hz, 1H), 2.35 (s, 3H), 1.66 (s, 9H), 1.14 (s, 9H). $^{13}\text{C NMR}$ (126 MHz, CDCl_3): δ 152.47, 150.04, 140.04, 136.35, 130.17, 129.59, 126.71, 125.83, 125.08, 124.24, 121.16, 108.33, 104.71, 104.18, 83.68, 69.11, 58.30, 55.92, 53.65, 51.94, 29.84, 28.33, 27.04, 19.46. ESI ($M + H$) $^+ = 481$.

General Procedure for the Synthesis of 39–41. To a room-temperature solution of **12** (1 equiv) in *i*-PrOH was added Et_2NH (20 equiv). The reaction mixture was sealed and heated to 150 °C overnight. The mixture was concentrated *in vacuo* and purified on silica gel (DCM/EA) to give the desired product **39–41**.

3-((1H-Indol-4-yl)oxy)-N-(tert-butyl)-2-methoxy-N-(4-methylbenzyl)propan-1-amine (39). White solid, $R_f = 0.3$ (DCM/EA = 3:1). $^1\text{H NMR}$ (500 MHz, CDCl_3): δ 8.12 (s, 1H), 7.24 (s, 1H), 7.10–7.04 (m, 4H), 7.00 (d, $J = 8.2$ Hz, 1H), 6.61 (t, $J = 2.3$ Hz, 1H), 6.34 (d, $J = 7.6$ Hz, 1H), 4.11 (dd, $J = 10.0, 3.2$ Hz, 1H), 3.81 (dd, $J = 10.0, 6.0$ Hz, 1H), 3.76–3.68 (m, 2H), 3.39 (s, 3H), 3.37–3.34 (m, 1H), 2.87 (dd, $J = 13.9, 8.2$ Hz, 1H), 2.75 (dd, $J = 13.9, 5.1$ Hz, 1H), 2.32 (s, 3H), 1.13 (s, 9H). $^{13}\text{C NMR}$ (126 MHz, CDCl_3): δ 152.96, 140.06, 137.38, 136.03, 128.98, 128.33, 122.85, 122.41, 119.00, 104.31, 100.72, 100.42, 80.10, 69.17, 58.40, 55.75, 55.67, 52.61, 27.42, 21.21. HRMS (ESI $^+$) m/z : [$M + H$] $^+$, calcd for $\text{C}_{24}\text{H}_{33}\text{N}_2\text{O}_2$, 381.2537; found, 381.2540.

1-((1H-Indol-4-yl)oxy)-3-((4-methylbenzyl)amino)propan-2-ol (37). To a room-temperature solution of **11d** (1 equiv) in *i*-PrOH was added Et_2NH (20 equiv). The reaction mixture was sealed and heated to 150 °C overnight. The mixture was concentrated *in vacuo* and purified on silica gel (DCM/EA) to give **1-((1H-indol-4-yl)oxy)-3-((4-methylbenzyl)amino)propan-2-ol (37)** as a colorless solid. $^1\text{H NMR}$ (400 MHz, chloroform-*d*): δ 8.28 (s, 1H), 7.23 (d, $J = 7.9$ Hz, 2H), 7.15 (d, $J = 7.8$ Hz, 2H), 7.12–7.06 (m, 2H), 7.03 (d, $J = 8.2$ Hz, 1H), 6.65–6.60 (m, 1H), 6.51 (d, $J = 7.5$ Hz, 1H), 4.24–4.16 (m, 1H), 4.17–4.08 (m, 2H), 3.88–3.77 (m, 2H), 3.01–2.82 (m, 2H), 2.62 (s, 2H), 2.34 (s, 3H). $^{13}\text{C NMR}$ (126 MHz, chloroform-*d*): δ 152.44, 137.45, 137.05, 136.83, 129.29, 128.25, 122.85, 122.84, 118.85, 104.93, 100.96, 99.95, 70.75, 68.69, 53.71, 51.44, 21.23. HRMS (ESI $^+$) m/z : [$M + H$] $^+$, calcd for $\text{C}_{19}\text{H}_{23}\text{N}_2\text{O}_2$, 311.1754; found, 311.1767.

tert-Butyl 4-(3-Bromopropoxy)-1H-indole-1-carboxylate (13). To a solution of **9** (1 equiv) in THF cooled to 0 °C was added NaH (1.5 equiv) in one portion. The reaction mixture was stirred at 0 °C for 1 h before, and then, 1,3-dibromopropane (1.5 equiv) was added dropwise. The mixture was allowed to warm to room temperature overnight with stirring. The reaction mixture was quenched with saturated aqueous NH_4Cl solution and extracted with EA. The organic layer was washed with saturated sodium bicarbonate solution, brine, dried (Na_2SO_4), and concentrated *in vacuo*. The crude residue was purified on silica gel to give the desired product **13** as a colorless solid. $^1\text{H NMR}$ (600 MHz, CDCl_3): δ 7.77 (d, $J = 7.2$ Hz, 1H), 7.51 (d, $J = 3.1$ Hz, 1H), 7.23 (t, $J = 8.1$ Hz, 1H), 6.69 (d, $J = 2.7$ Hz, 1H), 6.68 (s, 1H), 4.25 (t, $J = 5.8$ Hz, 2H), 3.66 (t, $J = 6.5$ Hz, 2H), 2.40 (p, $J = 6.2$ Hz, 2H), 1.68 (s, 9H). $^{13}\text{C NMR}$ (126 MHz, CDCl_3): δ

152.03, 149.96, 136.68, 125.18, 124.57, 121.11, 108.71, 104.29, 104.22, 83.81, 65.69, 32.61, 30.18, 28.31. EI ($M + H$) $^+ = 354$.

3-((1H-Indol-4-yl)oxy)-N-(tert-butyl)-N-(4-methylbenzyl)propan-1-amine (42). To a solution of **13** (1 equiv) in *i*-PrOH was added amine **14** (1.5 equiv). The mixture was sealed and heated to 120 °C overnight and then cooled and concentrated *in vacuo* and purified on silica gel to afford **3-((1H-indol-4-yl)oxy)-N-(tert-butyl)-N-(4-methylbenzyl)propan-1-amine (42)** as an off-white solid. $^1\text{H NMR}$ (600 MHz, CDCl_3): δ 8.10 (s, 1H), 7.34 (d, $J = 7.8$ Hz, 2H), 7.16–7.07 (m, 4H), 6.99 (d, $J = 8.2$ Hz, 1H), 6.65 (t, $J = 2.8$ Hz, 1H), 6.44 (d, $J = 7.7$ Hz, 1H), 4.01 (t, $J = 6.1$ Hz, 2H), 3.73 (s, 2H), 2.85 (t, $J = 7.2$ Hz, 2H), 2.37 (s, 3H), 1.85–1.80 (m, 2H), 1.18 (s, 9H). $^{13}\text{C NMR}$ (126 MHz, CDCl_3): δ 158.72, 152.64, 137.40, 133.79, 129.60, 122.77, 122.66, 118.83, 114.01, 104.66, 100.77, 100.00, 70.45, 67.45, 55.87, 55.32, 55.16, 53.92, 27.58. HRMS (ESI $^+$) m/z : [$M + H$] $^+$, calcd for $\text{C}_{23}\text{H}_{31}\text{N}_2\text{O}^+$, 351.2431; found, 351.2431.

Animal Procedures. All mice were purchased from Jackson Laboratories and housed under a 12 h light/12 h dark cycle at 22 °C. Before handling, mice were acclimated for at least 1 week in our animal facility. For drug administration, compounds were re-suspended in a 10% DMSO/10% Tween 80/80% phosphate-buffered saline solution at a final concentration of 10 mg/mL and was administered by intraperitoneal injection at 5 $\mu\text{L/g}$ body weight. Compounds were injected a total of three times. For overnight fast, food was removed after the second injection, and on the following morning (~ 9 a.m.), a third injection was administered and blood glucose was measured 3 h after the last injection. For 6 h fast, the third injection was given in the morning (~ 9 a.m.) and mice were fasted for 6 h following the last injection before blood glucose was measured. Glycemia was measured by tail bleed using a glucometer (OneTouch). For all experiments, age- and body weight-matched animals were used. For protein extracts and biochemistry studies, tissues were removed following each experiment and snap-frozen in liquid nitrogen. All studies were performed according to protocols approved by Beth Israel Deaconess Medical Center's Animal Care and Use Committee.

Glucose Production Assay. Primary hepatocytes were isolated from 8- to 12-week-old male C57BL/6 mice by perfusion with the liver digest medium (Invitrogen, 17703-034), followed by 70 μm mesh filtration. Percoll (Sigma, P7828) gradient centrifugation allowed primary hepatocyte isolation from other cell types and debris. Cells were seeded in the plating medium [Dulbecco's modified Eagle's medium (DMEM) with 10% fetal bovine serum (FBS), 2 mM sodium pyruvate, 1% penicillin/streptomycin, 1 μM dexamethasone, and 100 nM insulin]. After 4 h of seeding, the medium was changed and incubated in the maintenance medium [DMEM with 0.2% bovine serum albumin (BSA), 2 mM sodium pyruvate, 1% penicillin/streptomycin, 0.1 μM dexamethasone, and 1 nM insulin]. The following day (day 1), hepatocytes were treated overnight with the indicated compounds at 1 μM . On day 2, media were changed to glucose production media (glucose-free DMEM with 0.2% BSA, 20 mM sodium pyruvate, 2 mM sodium lactate, 1% penicillin/streptomycin, 4 mM glutamine, and sodium bicarbonate) supplemented with glucagon (200 nM) and fresh compounds. After 4 h of incubation, media were collected and the glucose level was measured using a glucose assay kit from Eton Bioscience Inc.

Lipolysis Assay. Immortalized brown adipocytes were allowed to differentiate for 5–7 days in the differentiating medium (DMEM with 10% FBS, 1 μM rosiglitazone, 0.5 mM 3-isobutyl-1-methylxanthine, 5 μM dexamethasone, 20 nM insulin, and 1 nM T3). Upon differentiation, the medium was changed to DMEM containing 2% BSA, and cells were immediately treated with the indicated compounds for 30 min and then stimulated with NE (1 μM) for additional 90 min. The medium was collected, and glycerol levels secreted to the medium were measured using the free glycerol reagent (Sigma, F-6428).

Liver Glycogen Measurement. ~ 50 mg of the pulverized liver was homogenized in 6% perchloric acid, and the homogenate was centrifuged for 10 min at $\times 13,000g$ at 4 °C and neutralized with KHCO_3 . The supernatant was subjected to amyloglucosidase

digestion (0.5 mg/mL in 0.2 M acetate, pH = 4.8) for 1 h at 37 °C. Following digestion, the glucose concentration was measured using a glucose measurement kit (Eton Bioscience Inc.). Glucose levels of the pre-amyloglucosidase-digested samples were subtracted to determine glycogen levels.

■ ASSOCIATED CONTENT

Supporting Information

The Supporting Information is available free of charge at <https://pubs.acs.org/doi/10.1021/acs.jmedchem.0c01450>.

HPLC analysis results of target compounds (PDF)

Molecular formula strings with biological data (CSV)

■ AUTHOR INFORMATION

Corresponding Author

Theodore M. Kamenecka – Department of Molecular Medicine, The Scripps Research Institute, Jupiter, Florida 33458, United States; orcid.org/0000-0002-3077-0167; Phone: 561-228-2207; Email: kameneck@scripps.edu

Authors

Hua Lin – Department of Molecular Medicine, The Scripps Research Institute, Jupiter, Florida 33458, United States; Biomedical Research Center of South China, College of Life Sciences, Fujian Normal University, Fuzhou 350117, China; orcid.org/0000-0002-0840-6553

Kfir Sharabi – Department of Cancer Biology, Dana-Farber Cancer Institute, Boston, Massachusetts 02215, United States; Department of Cell Biology, Harvard Medical School, Boston, Massachusetts 02115, United States

Li Lin – Department of Molecular Medicine, The Scripps Research Institute, Jupiter, Florida 33458, United States

Claudia Ruiz – Department of Molecular Medicine, The Scripps Research Institute, Jupiter, Florida 33458, United States

Di Zhu – Department of Molecular Medicine, The Scripps Research Institute, Jupiter, Florida 33458, United States

Michael D. Cameron – Department of Molecular Medicine, The Scripps Research Institute, Jupiter, Florida 33458, United States

Scott J. Novick – Department of Molecular Medicine, The Scripps Research Institute, Jupiter, Florida 33458, United States

Patrick R. Griffin – Department of Molecular Medicine, The Scripps Research Institute, Jupiter, Florida 33458, United States; orcid.org/0000-0002-3404-690X

Pere Puigserver – Department of Cancer Biology, Dana-Farber Cancer Institute, Boston, Massachusetts 02215, United States; Department of Cell Biology, Harvard Medical School, Boston, Massachusetts 02115, United States

Complete contact information is available at:

<https://pubs.acs.org/doi/10.1021/acs.jmedchem.0c01450>

Author Contributions

H.L. and K.S. contributed equally. The manuscript was written through contributions of all authors. All authors have given approval to the final version of the manuscript.

Notes

The authors declare no competing financial interest.

■ ACKNOWLEDGMENTS

This work was supported by a Charles King Postdoctoral Fellowship to K.S. and by the National Institute of Diabetes and Digestive and Kidney Diseases, USA (DK117655 to P.P. and P.R.G.). K_i determinations, receptor binding profiles, and agonist and/or antagonist functional data were generously provided by the National Institute of Mental Health's Psychoactive Drug Screening Program, Contract # HHSN-271-2018-00023-C (NIMH PDSP). The NIMH PDSP is directed by Bryan L. Roth MD, Ph.D, at the University of North Carolina at Chapel Hill and Project Officer Jamie Driscoll at NIMH, Bethesda MD, USA.

■ ABBREVIATIONS

T2D, type 2 diabetes; HGP, hepatic glucose production; SAR, structure–activity relationship; PGC-1 α , peroxisome proliferator-activated receptor gamma coactivator 1-alpha; β -AdR, β -adrenergic receptor; TZDs, thiazolidinediones; SGLT2, sodium-glucose cotransporter 2; SHT1a, 5-hydroxytryptamine receptor 1a; MeOH, methanol; EtOH, ethanol; CH₃CN, acetonitrile; Boc, *t*-butoxycarbonyl; DMF, dimethylformamide; 4-DMAP, 4-dimethylaminopyridine; DCM, dichloromethane; DIPEA, *N,N*-diisopropylethylamine; NE, norepinephrine; SGIGP, suppression of glucagon-induced glucose production; SNIL, suppression of norepinephrine-induced lipolysis; HSL, hormone-sensitive lipase; HFD, high fat diet

■ REFERENCES

- (1) Sharabi, K.; Tavares, C. D. J.; Rines, A. K.; Puigserver, P. Molecular pathophysiology of hepatic glucose production. *Mol. Aspects Med.* **2015**, *46*, 21–33.
- (2) Moore, M. C.; Coate, K. C.; Winnick, J. J.; An, Z.; Cherrington, A. D. Regulation of hepatic glucose uptake and storage in vivo. *Adv. Nutr.* **2012**, *3*, 286–294.
- (3) Lin, H. V.; Accili, D. Hormonal regulation of hepatic glucose production in health and disease. *Cell Metab.* **2011**, *14*, 9–19.
- (4) Deacon, C. F. Dipeptidyl peptidase-4 inhibitors in the treatment of type 2 diabetes: a comparative review. *Diabetes, Obes. Metab.* **2011**, *13*, 7–18.
- (5) Bailey, T. Options for combination therapy in type 2 diabetes: comparison of the ADA/EASD position statement and AACE/ACE algorithm. *Am. J. Med.* **2013**, *126*, S10–S20.
- (6) Magnusson, I.; Rothman, D. L.; Katz, L. D.; Shulman, R. G.; Shulman, G. I. Increased rate of gluconeogenesis in type II diabetes mellitus. A ¹³C nuclear magnetic resonance study. *J. Clin. Invest.* **1992**, *90*, 1323–1327.
- (7) Consoli, A.; Nurjhan, N.; Capani, F.; Gerich, J. Predominant role of gluconeogenesis in increased hepatic glucose production in NIDDM. *Diabetes* **1989**, *38*, 550–557.
- (8) Rojas, L. B. A.; Gomes, M. B. Metformin: an old but still the best treatment for type 2 diabetes. *Diabetol. Metab. Syndr.* **2013**, *5*, 6.
- (9) Pernicova, I.; Korbonits, M. Metformin—mode of action and clinical implications for diabetes and cancer. *Nat. Rev. Endocrinol.* **2014**, *10*, 143–156.
- (10) Hundal, R. S.; Krssak, M.; Dufour, S.; Laurent, D.; Lebon, V.; Chandramouli, V.; Inzucchi, S. E.; Schumann, W. C.; Petersen, K. F.; Landau, B. R.; Shulman, G. I. Mechanism by which metformin reduces glucose production in type 2 diabetes. *Diabetes* **2000**, *49*, 2063–2069.
- (11) Yoon, J. C.; Puigserver, P.; Chen, G.; Donovan, J.; Wu, Z.; Rhee, J.; Adelmant, G.; Stafford, J.; Kahn, C. R.; Granner, D. K.; Newgard, C. B.; Spiegelman, B. M. Control of hepatic gluconeogenesis through the transcriptional coactivator PGC-1. *Nature* **2001**, *413*, 131–138.
- (12) Puigserver, P.; Rhee, J.; Donovan, J.; Walkey, C. J.; Yoon, J. C.; Oriente, F.; Kitamura, Y.; Altomonte, J.; Dong, H.; Accili, D.;

Spiegelman, B. M. Insulin-regulated hepatic gluconeogenesis through FOXO1-PGC-1 α interaction. *Nature* **2003**, *423*, 550–555.

(13) Herzig, S.; Long, F.; Jhala, U.; et al. CREB regulates hepatic gluconeogenesis through the coactivator PGC-1. *Nature* **2001**, *413*, 179–183.

(14) Rodgers, J. T.; Lerin, C.; Haas, W.; Gygi, S. P.; Spiegelman, B. M.; Puigserver, P. Nutrient control of glucose homeostasis through a complex of PGC-1 α and SIRT1. *Nature* **2005**, *434*, 113–118.

(15) Rodgers, J. T.; Haas, W.; Gygi, S. P.; Puigserver, P. Cdc2-like kinase 2 is an insulin-regulated suppressor of hepatic gluconeogenesis. *Cell Metab.* **2010**, *11*, 23–34.

(16) Lerin, C.; Rodgers, J. T.; Kalume, D. E.; Kim, S.-h.; Pandey, A.; Puigserver, P. GCN5 acetyltransferase complex controls glucose metabolism through transcriptional repression of PGC-1 α . *Cell Metab.* **2006**, *3*, 429–438.

(17) Dominy, J. E., Jr.; Lee, Y.; Jedrychowski, M. P.; Chim, H.; Jurczak, M. J.; Camporez, J. P.; Ruan, H.-B.; Feldman, J.; Pierce, K.; Mostoslavsky, R.; Denu, J. M.; Clish, C. B.; Yang, X.; Shulman, G. I.; Gygi, S. P.; Puigserver, P. The deacetylase Sirt6 activates the acetyltransferase GCN5 and suppresses hepatic gluconeogenesis. *Mol. Cell* **2012**, *48*, 900–913.

(18) Sharabi, K.; Lin, H.; Tavares, C. D. J.; Dominy, J. E.; Camporez, J. P.; Perry, R. J.; Schilling, R.; Rines, A. K.; Lee, J.; Hickey, M.; Bennion, M.; Palmer, M.; Nag, P. P.; Bittker, J. A.; Perez, J.; Jedrychowski, M. P.; Ozcan, U.; Gygi, S. P.; Kamenecka, T. M.; Shulman, G. I.; Schreiber, S. L.; Griffin, P. R.; Puigserver, P. Selective chemical inhibition of PGC-1 α gluconeogenic activity ameliorates Type 2 diabetes. *Cell* **2017**, *169*, 148–160.

(19) Tejani-Butt, S. M.; Brunswick, D. J. Synthesis and beta-adrenergic receptor blocking potency of 1-(substituted amino)-3-(4-indolyloxy)propan-2-ols. *J. Med. Chem.* **1986**, *29*, 1524–1527.

(20) Blondeau, D.; Sliwa, H.; Deceaurriz, C. Beta-Adrenergic blocking activity of an indolizine analog of pindolol. *Eur. J. Med. Chem.* **1978**, *13*, 576.

(21) Besnard, J.; Ruda, G. F.; Setola, V.; Abecassis, K.; Rodriguiz, R. M.; Huang, X.-P.; Norval, S.; Sassano, M. F.; Shin, A. I.; Webster, L. A.; Simeons, F. R. C.; Stojanovski, L.; Prat, A.; Seidah, N. G.; Constam, D. B.; Bickerton, G. R.; Read, K. D.; Wetsel, W. C.; Gilbert, I. H.; Roth, B. L.; Hopkins, A. L. Automated design of ligands to polypharmacological profiles. *Nature* **2012**, *492*, 215–220.

(22) Sharabi, K.; Tavares, C. D. J.; Rines, A. K.; Puigserver, P. Molecular pathophysiology of hepatic glucose production. *Mol. Aspects Med.* **2015**, *46*, 21–33.

(23) Krushinski, J. H., Jr.; Schaus, J. M.; Thompson, D. C.; Calligaro, D. O.; Nelson, D. L.; Luecke, S. H.; Wainscott, D. B.; Wong, D. T. Indoloxypyropanolamine analogues as 5-HT(1A) receptor antagonists. *Bioorg. Med. Chem. Lett.* **2007**, *17*, 5600–5604.

(24) Ogradowczyk, M.; Dettlaff, K.; Jelinska, A. Beta-Blockers: current state of knowledge and perspectives. *Mini-Rev. Med. Chem.* **2016**, *16*, 40–54.

(25) Duncan, R. E.; Ahmadian, M.; Jaworski, K.; Sarkadi-Nagy, E.; Sul, H. S. Regulation of lipolysis in adipocytes. *Annu. Rev. Nutr.* **2007**, *27*, 79–101.

(26) Han, H.-S.; Kang, G.; Kim, J. S.; Choi, B. H.; Koo, S.-H. Regulation of glucose metabolism from a liver-centric perspective. *Exp. Mol. Med.* **2016**, *48*, No. e218.